UNIVERSITY OF PARDUBICE

FACULTY OF CHEMICAL TECHNOLOGY

Department of Graphic Arts and Photophysics

Optical Properties of Thin Colored Layers

Literature Survey

2006

Table of content

1.   Introduction

Almost all materials found in daily life contain color components. Better understanding of colorant properties and their effect on ink layer formulation and color appearance enable to provide higher quality products. Theory that would answer the question how the substrate properties, components, thickness of the bulk and other factor affect the optical properties of resulting material is in interest in many disciplines [1, 2, 3]. The theory must be capable to of predicting the fraction of light reflected from the surface exposed to radiation from all directions in hemisphere [1].

In the past significant amount of attempts for theories that relate the physical properties with scattering and absorption properties of particle was developed. Some of them proved to be good approximation, others exhibit week assumptions. In printing, textile and dye industry the most popular is the two fluxes Kubelka-Munk approach and its extensions including surface correction. Other more complex methods have been published by number of authors [1]. For halftone assessment Neugebauer equations, Yule-Nielsen approximation and Clapper-Yule multiple internal reflections has been widely adopted and further enhanced [4].

Photoacoustic is versatile technique for non-destructive investigation of wide range of samples including solids, powers, gases, suspensions, emulsions [5]. It enables to study absorption spectra of scattering samples where common transmission methods fail.

The PA technique developed by Rosenweig and Gersho has been found to be reasonable, however, modification for light scattering phenomenon was necessary. Kubelka-Munk approach has been considered but has been found to be of limited use in explanation the effect of light scattering on PA response. Other factor such as surface area and energy transfer of heat from solid to gas are more important in quantifying the effect of particle size and light scattering on PA signal [6].

2. Optics of colored layers

2.1. Interaction of light with material

The process of light interaction that is schematically shown in figure 1 includes reflection at surface, scattering or absorption of the light passing through the matter and transmission. Another mechanism called fluorescence refers to re-emission of absorbed light. Due to the character of paint layer fluorescence will be ignored. The relation between incident, reflected, transmitted and scattered light can be expressed:

$$I_0 = I_r + I_s + I_a + I_t \quad \text{or} \tag{1}$$

$$1 = R + S + A + T$$

Where I_0 denotes the incident intensity, I_r, I_s, I_a, I_t are amounts of reflected, scattered, absorbed and transmitted light respectively. R, S, A, T are the fraction of light interacting by appropriate mechanism [7].
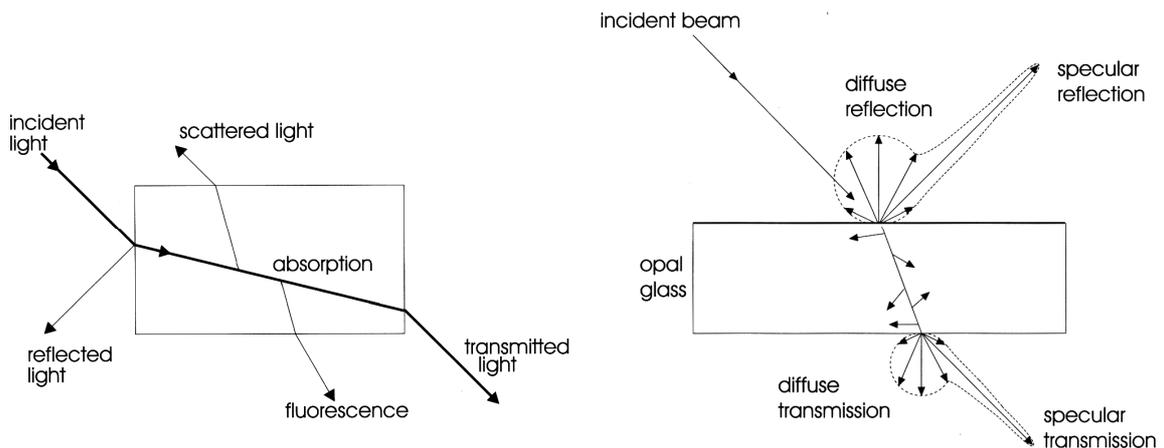
Figure 1: Light interaction with matter [7]

2.2. Transmissions

2.2.1. Direct (specular) transmission

When light impinge on polished glass surface small amount of light, the specular component, is reflected at the angle of incidence but most of the light enter the glass and following the laws of refraction changes the direction. The refraction phenomena can be described by Snell's Law:

$$n_1 \sin \Theta_1 = n_2 \sin \Theta_2 \tag{2}$$

where Θ_1, Θ_2 is the angle of incidence and refraction respectively and n_1 is the refractive index of medium outside glass and n_2 of glass. As the refractive index of air is close to unity we usually assume the n_1 to be unite [8, 9].

The light passing trough the glass is partly absorbed and at the second interface of glass plate and considered media where is again decreased by specular reflection emerge [10].

2.2.2. Diffuse transmissions

The passage of light through perfectly transparent glass described above is somehow idealised, in practice transmission is always followed by scattering causing some of the transmitted light emerges the medium in direction quite different from the original path. Scattering of light occurs:

> a) on smooth polished surfaces,
>
> b) through shape irregularities,
>
> c) due to the interaction of light with impurities with different refractive index presented in material.

Scattering on smooth polished surfaces originate from light reflection on micro-scratches that comes from the polishing process itself. Light scattering of type *b* can be observed in ground glass that has irregular surfaces. Opal glass with different refractive index infusion gives arise of type *c* scattering.

For high polished optical glass the components *a* and *b* are negligible and *c* will be zero. Materials like tissue paper with pronounced structure will show large amount of scattering of type *b* and *c* and transmission will be almost diffuse [10].

2.3. Absorption

Usually, when measuring transmittance it is more preferable to use logarithmic scale instead of direct transmittance factor. If we assume the absorption originate from absorption centres such as dye molecules, transition metal ions or small metal particles being uniformly distributed through the material then the amount of light absorbed in plate is given by:

$$I = I_0 e^{-\alpha_a l} \tag{3}$$

where I is the fraction of light emerging from the plate, I_0 denotes incident irradiance and l is thickness of plate, and α_a is the linear absorption coefficient. This description of absorption theory applies only to single wavelength and is known as Lambert's law.

Consideration that absorption is proportional to absorption centres of specimen is figure in Beer-Lambert law:

$$\log(I/I_0) = \varepsilon[J]l \tag{4}$$

where I is the intensity of light after passage through the length l, I_0 denotes incident irradiance and $[J]$ is molar concentration of absorbing species and ε is called molar absorption or extinction coefficient. If A now stands for the product $\varepsilon[J]l$ and the ratio I/I_0 is the measure of transmission T we can write:

$$log_{10} \, T = A \tag{5}$$

The reason why absorbance is used rather than transmittance factor is the linear relationship between concentration and absorbance.

If different species of known absorption characteristics are mixed then absorbance measurements at different wavelengths arrange determination of concentration of each colorant in the specimen without need to separate them chemically [10, 7].

2.4. Reflections

Reflectance is a dominant mechanism at appearance of solid [7]. The term reflectance refers to all interaction processes of light with matter in which photons are send back into the hemisphere of incident light [9]. There are two types of reflection differing by the angle at which the reflected beam leaving the surface: specular as was indicated in chapter 2. 2. 1 and diffuse.

2.4.1. Diffuse reflections

Diffuse reflections occur on rough surface when light emerges from the surface at myriad different directions. It grows with increasing surface roughness. Diffuse reflection is feature of ideal matt paint. Most realistic object exhibit both type of reflection, the proportion of relative amount of diffuse to specular reflectance is measure of gloss [10, 7].

2.4.2. Specular reflection

Specular component features the reflected angle being equal to that of incidence as mentioned in chapter 2. 2. 1. This mirror like reflection is dominant for paint, which resembles liquid and shows the gloss on polished surfaces [10].

Measurement of reflectance

In Graphic Arts reflectance measurement are basic in evaluation quality of printed samples. Reflectance spectra can be used for determination of color coordinates such as L*a*b* or XYZ by multiplying the spectra by appropriate illuminant characteristics and observer weighting function with subsequent summation. Similarly, if spectral composition of appropriate filter is used density calculation and further densitometric characteristics such as dot area determination can be done.

Reflectance measurements are usually performed in comparison with perfect reflecting diffuser. This can be specially developed white tiles, white plastics materials or block of magnesium carbonate.

The so-called reflectance factor of surface is ratio of visible radiation reflected form it and that reflected from the perfect diffuser at given condition [10].

Another important issue in reflectance determination are the conditions of measurement. Since most printing substrates are translucent, the reflectance of printed sample is influenced by optical properties of material that is below the measured sheet. The background together with opacity of the material being measured is pivotal in regard what will happen with the light passing through the paper and striking the backing material, thus black backing selection involve great care [11].

The light scattering and reflection in substrate has been investigated by F. P. Callaham [12] who proposed that the effect of sideways scattering in substrate on half tone densities is negligible for practical application. On the contrary, study by F. R. Clapper and J. A. C. Yule led to opposite conclusion. They suggest effect of multiple internal light reflections on the densities of halftone prints can almost halve the reflectance. The internal reflection in paper has to be treated together with light scattering, because for given solid ink density there would be no effect of internal reflection in absence of light scattering.

The incident light may follow quite complex path in being reflected or absorbed by paper. Each times it strikes the paper surface it enters the halftone pattern and may be absorbed. The non-absorbed part can be reflected back or transmitted through the surface. Total reflectance is given by sum of all portions emerging from the surface at each cycle.

From the light that impinge on the sample surface part r_s is being reflected at first surface reflection, the rest *1 - r_s* penetrates through ink film into paper of which fraction a will enter through the printed dot and *1 - a* through clear area (see figure 2). Summarization of the light passing trough these two ways with respect of *t* being the transmittance gives *1 - a + at*. Irradiance in the paper given by the light penetrating is *(1 - r_s)(1 – a + at)*. At the paper second (bottom) surface a fraction *r* is reflected back and continues way through paper.

Incident Irradiance

1st Surface reflectance

1st Emergence

$x(1 - a)(1-r_s)(1-a+at)r$
$= x(1-r_s)(1-a+at)r$
$xat(1-r_s)(1-a+at)r$

Fr_s

(n-1)r$_s$t Emergence

$x(1-a)b$
$= x(1-a+at)b$
$xatb$

nth Emergence

$x(1-a)(1-x)(1-a+at+at^2)rb$
$= x(1-x)(1-a+at+at^2)rb$
$xat(1-x)(1-a+at+at^2)rb$

$(1-r_s)(1-a)$

$(1-r_s)at$

$(1-r_s)(1-a+at)r$

$(1-r_s)(1-a+at)r(1-x)(1-a)$

$(1-r_s)(1-a+at)r(1-x)at^2$

$(1-r_s)(1-a+at)(1-x)r^2(1-a+at^2)$

a

b

$(1-a)(1-x)b$

$at^2(1-x)b$
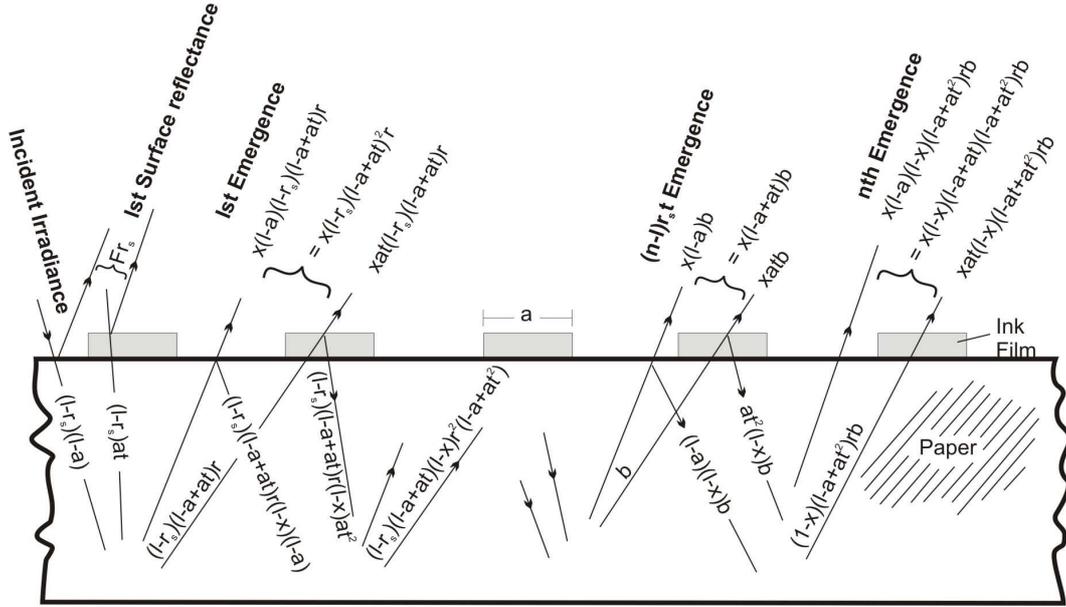
$(1-x)(1-a+at^2)rb$

Ink Film

Paper

Figure 2: Sideways scattering and internal reflections within halftone sample [14]

Where this passing light hit the clear area of printed sample $x(1 - a)(1 - r_s)(1 - a + a)r$ emerges and $(1 - x)(1 - a)(1 - rs)(1 - a + a)r$ is reflected back into paper. Similarly, where the light strike the dot pattern $xat(1 - r_s)(1 - a + a)r$ comes out and $at^2(1 - x)(1 - r_s)(1 - a + a)r$ is reversed in direction and passage again through the paper. Factor x is related to reflective index of paper, $1 - x$ equal to reflectance of internally incident diffuse light at air surface. This process take over each cycle the light makes the attempt to emerge from the matter.

The light emerging at:

first cycle = $rx (1 - r_s)(1 - a + at)^2$ (6)

second cycle = $rx (1 - r_s)(1 - a + at)^2 \times [r(1 - r_s)(1 - a + at^2)]$ (7)

n^{th} cycle = $rx (1 - r_s)(1 - a + at)^2 \times [r^{n-1}(1 - r_s)^{n-1} (1 - a + at^2)]^{n-1}$ (8)

first surface reflection = Fr_s (9)

Total reflectance is given by summarization of light emerging at each cycle as compared to with a perfect diffuser reflector:

$$R = Fr_s + \frac{x(1 - r_s)r(1 - a + at)^2}{1 - r(1 - x)(1 - a + at^2)}$$ (10)

If the reflectance is measured in relation to paper:

$$R = \frac{\dfrac{Fr_s}{1 - r_s} + \dfrac{xr(1 - a + at)^2}{1 - r(1 - x)(1 - a + at^2)}}{(Fr_s / 1 - r_s) + [rx / 1 - r(1 - x)]}$$ (11)

where $Fr_s + [x(1 - r_s)r/1 - r(1 - x)]$ denotes the reflection of unprinted paper.

In case the paper is perfectly white, r equals 1 and thus the expressions simplifies:

$$R = \frac{\dfrac{Fr_s}{1-r_s} + \dfrac{x(1-a+at)^2}{1-r(1-x)(1-a+at^2)}}{(Fr_s/1-r_s)+1} \qquad (12)$$

The solid where $a = 1$ follows:

$$R = \frac{\dfrac{Fr_s}{1-r_s} + \dfrac{xt^2}{1-(1-x)t^2}}{(Fr_s/1-r_s)+1} \qquad (13)$$

Further calculations for specific condition assuming 40 % of light escaping and 60 % reflected back each time the light encounter the paper surface [13] and restricted to perfectly white paper with $r = 1$ has been performed [14]. F. R. Clapper and J. A. C. Yule came to the conclusion that in extreme case – fine screening, translucent paper – multiple internal reflection can result in density three times higher than of that predicted from the simple formula dot area calculation.

2.5. Light scattering

Light absorption that refers to reduction of light intensity is sometimes mixed with light scattering. The basic difference is that true absorption is connected with transformation of the radiation energy into another kind of energy such as thermal whereas scattering not. Light scattering refers to all physical process that move photon apart in different direction. As indicated in chapter 2. 2. 2 in practice the scattering is often caused by local impurities of refractive index or shape irregularities. Further scattering caused by small particles dispersed in homogenous medium will be discussed. Other mechanisms of ray scattering as for instance Raman will not be consider as they are rare in nature.

Let us concentrate on thin element of thickness dx of that media. The lost of light dI due to passage through the slide of thickness dx is proportional to the flux intensity I:

$$dI = -k(\lambda)Idx \qquad (14)$$

the integration results in:

$$I = I_0 e^{kx} \qquad (15)$$

where $k(\lambda)$ is light scattering coefficient of medium for given wavelength. The integrated equation is analogical to Lambert formula, but instead of light absorption centres now scattering centres are employed.

The scattering coefficient depends on:

- concentration of scattering centres,

- relation of particle size to wavelength of incident light,

- differences between particles and medium in which they are distributed,

- particle shape.

The relation of light scattering phenomena on particle size is found by leaving the remaining factor constant. The dependency illustrated in figure 3 shows that the maximum scattering power occurs when particle dimension is somewhat less than wavelength of the light interacting.
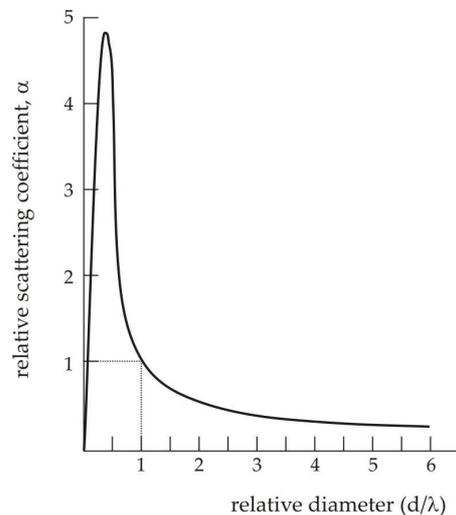

Figure 3: Dependency of scattering coefficient on particle size [7]

The effect of above listed items such as concentration and particle/medium refractive index on light scattering is widely utilized in industry. For example many plastics are made opacity by adding white pigment with high refractive index. This issue will be discussed in detail in chapter 3. 2. [7, 9].

2.5.1. Rayleigh scattering

During 19th century number of studies dealt with light scattering by small particles. Keen and Porter [15] carry out experiments in which they evaluated color and intensity of light transmitted through suspension of precipitated-sulphur-particle with dimension comparable or decidedly larger than wavelength of light.

Tyndall [7] has observed suspension of water with small addition of milk illuminated by white light that appear bluish when viewed from side whereas the emerging light exhibit red

tint. He has suggested that blue light is more strongly scattered than the red and thus this blue scattering is referred as Tyndall blue.

The effect of scattering was mathematically characterized by Rayleigh who has investigated the diffraction of light by spheres of small relative index and transmission of light through an atmosphere containing small particles in suspension [16]. He further show that even fluctuation of refractive index in otherwise homogenous material can give arise scattering. The Rayleigh theory applies to independent scattering on speherical shells with diameter about ten times smaller than wavelength of incident ray. For unpolarized light of intensity I_0 that is disturbed by scattering centre, the intensity of scattered light can be derived as following:

$$I_s = I_0 \left(\frac{9\pi^2 V^2}{2x^2 \lambda^4} \right) \left(\frac{m^2 - 1}{m^2 + 2} \right)^2 (1 + \cos^2 \theta) \qquad (16)$$

where x measure the distance at which the intensity I_s is determined, V is the volume of scattering species, θ is angle between direction of incident and scattered light and m denote the relative refractive index of particle:

$m = n_{particle} / n_{medium}$

The light is scattered backward as much as forward, but only half intensity is observed at angle $\theta = 90°$. As the formula shows the scattered light is proportional to $1/\lambda^4$. Thus as Tyndall has correctly suggested shorter wavelengths are more scattered than longer.

Further, comparison of experiments with theory reveals, that molecule alone can act as scattering centre, thus even the purest gas exhibits scattering. This finding enables to estimate molecular size and number of molecules in unit volume.
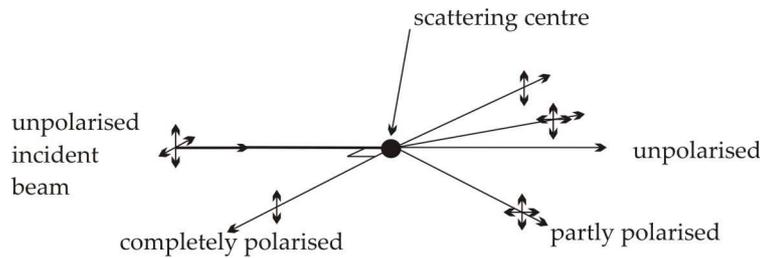

Figure 4: Distribution of scattered light polarisation [7]

The Rayleigh phenomenon is characterized by strongly polarized light. Two linearly polarized components are found. If x, y is plane of observation where x denotes the direction of primary ray then one with electric vector lying parallel to the x-y plane and second of which the electric field vector is orthogonal to plane of observation. The wave polarised perpendicularly to x-y plane is scattered equally in all direction. The intensity distribution of

the wave where the electric field vector is the plane *x-y* follows the dumbbell shape. The Rayleigh scattering pattern is given by summarization of both contributions.

The distribution of polarization is shown in figure 4. At the angle $\theta = 90°$ where only one polarization component is presented the light is perceived as completely linearly polarized. At the direction of primary ray ($\theta = 0$) and backward to primary beam ($\theta = 180°$) the light is unpolarised. In any other direction mixture of both polarizations occurs [7, 8].

3.   Properties of layers with colorants and paper

3.1. Gloss

Generally, the gloss is determined by the way in which the light interacts with the surface. As indicated in chapter 2. 4 gloss is measure of light that is reflected at the angle equal to that of incidence (specular angle) and competitive diffusely (randomly) reflected light. The greater proportion is reflected at the specular angle the glossier the surface appears [17].

As the pigment is the largest visible part of ink/coating film, it directly affects the gloss. Closer study by Jayasuriya et al. of gloss as a function of surface roughness from different aqueous coating on various paper substrates showed that the gloss decreases non-linearly with increasing surface roughness of pigmented layer [18].

Another factor contributing is the ratio of pigment and vehicle used in ink formulation. The more the pigment particles of the ink layer are covered by the binder the smoother and glossier the surface appears [19].

3.1.1. Printing media gloss

According to Tappi [20] standards gloss is defined as $75\degree$ spectral reflectance at 550 nm. Whereas print gloss being usually measured at 60 °angle.

Regardless the way it is measured, the print and paper gloss is important in interpreting printability of inkjet papers and image quality.

Chinamayanadam described gloss as a function of refractive index, incident light wavelength and surface roughness:

$$G = \frac{I}{I_0} = f(n,i)e^{-\left(\frac{4\pi\sigma\cos(i)}{\lambda}\right)^2} \qquad (18)$$

I and I_0 denote specularly reflected and incident light intensities, $f(n,i)$ is Fresnel coefficient of specular reflection as a function of refractive index n and angle of incident light. σ is standard deviation of surface roughness and λ is wavelength of incident light.

The printing media gloss depends on both the chemical and morphology properties of pigment used [21].

The possibility of use fumed metallic oxide pigments for ink jet papers coating and the effect of its properties to final coating quality was studied by Lee et al. [22] and Ramakrishan [16]. Results have shown that fumed metallic oxide pigments are capable to produce semi-gloss and high-gloss inkjet papers providing acceptable reproduction after calendaring. It was

demonstrated that the fumed alluminia pigments provided higher gloss than fumed silica. An important finding was the gloss grew with increasing particle size, which does not follow principles for conventional pigments. The gloss restriction with silica particle size reduction was explained by rise of crack in the coating cased by decreasing particle size.

Addition of larger pigments to fumed silica coating increases the substrate porosity enabling the coating to scatter more incidents light and thus intensify the brightness, gloss and opacity [21].

3.1.2. Ink layer gloss

Printing gloss is one aspect of printing quality assessment. Gloss intensify the appearance of color, except for the specular angle, as it reduces the colorless light reflected [17]. Recent studies showed its development to be complex process and depends on substrate and ink properties and printing conditions. As gloss is function of surface smoothness all processes leading to formulation of planar layers increase the gloss.

Interaction of ink with paper, namely ink penetration which reduce the gloss, is influenced by substrate properties including roughness, porosity and coating formulation (latex, mineral). Another factor is proportion of amount of vehicle and pigment. Generally the higher the ratio the smoother the surface.

The printing conditions relating ink flow between rollers, inks pressure profile and ink transfer to paper, ink thickness have been studied in past by number of authors. For example Enonae at al observed anisotropy at right angles to the print direction. Preston et al. found that fast setting coating exhibit in offset lithography micro rough surface and thus dropping down the gloss. Influence of physical and chemical drying mechanism of sheetfed ink on coated papers was developed by Strom and Gustafsson [23].

Gloss is to some extend related to pigment shape. Textured surfaces, pearlescent and metallic inks change the way in which the light is scattered or reflected and show different reflection characteristics in different direction. The flattened disc-like structure of HSP that acts as little mirrors and reflect the light specularly contributes to gloss and opacity as well. If the shell of HSP is thermoplastics the particles would be yet more flattened after the process of calendering where the paper passes through heated pressured sets of rollers thus more enhancing gloss [24].

3.2. Opacity (tinting strength, covering or hiding power)

Hiding power defines the power of coating to obliterate the surface. It depends on its absorbing and scattering properties that are the functions of thickness and pigment concentration. The color is also important factor.

The covering power is proportional to difference between refractive index of pigment and that of vehicle in which is dispersed. The higher the difference the higher the covering power is. However, the refractive index of commonly used pigments and binders being very similar, except TiO_2, means these pigments can provide satisfactory coating opacity only if the content exceeds the critical volume pigment concentration. In materials with pigment amount above critical pigment volume concentration (CPVC) the opacity comes from light scattering at air/pigment interfaces. Higher refractive index of TiO_2 is one of the reasons why TiO_2 is now so extensively used as white pigment in coating below CPVC [25, 26].

Hollow sphere synthetic (HSP) pigments with refractive index close to that of binder in high binder formulation where is no light scattering at air/pigment interfaces utilizing contribution of the encapsulated air voids. Mechanism of light scattering at the shell is demonstrated in figure 5.
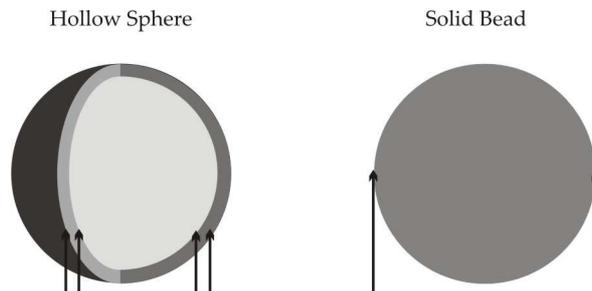

Figure 5.: Comparison of light scattering mechanism at Hollow Sphere and Solid Bead pigments [24]

The light scattering properties of HSP enables them to be widespread high quality paints and being capable to space TiO_2 [24].

3.3. Colorant mixtures

To provide whole range of hues needed individual dyes and pigments are mixed. When relating the concentration of components in mixture to the way the color is produced several situation can be distinguish. These include the simplest when the non-diffusing colorant are contained in transparent media, complicated situation if the layer with non-diffusing colorant are in contact with reflecting diffuser and the more complex case where the colorants except absorbing also diffuse the light [8].

3.3.1. Non-diffusing colorants in transmitting material

The color properties of non-diffusing particles can be easy characterized by spectral transmission. If we compare transmittance spectra for three different dye concentrations the curves course vary with colorant concentration in a quite complicated way (see figure 6). However, if transmission density spectra $D(\lambda)$ calculated as $D(\lambda) = log_{10}(1/T(\lambda))$ is plotted instead then the curves course is similar with the relation between them being multiplication by factor which is constant with wavelength. Finally if we calculate common logarithms of the transmission density spectra $D(\lambda)$, $log_{10}(1/D(\lambda))$, then the curves have same shape. Their separation on the $log_{10}(1/D(\lambda))$ axis is proportional to the dye/pigment concentration.
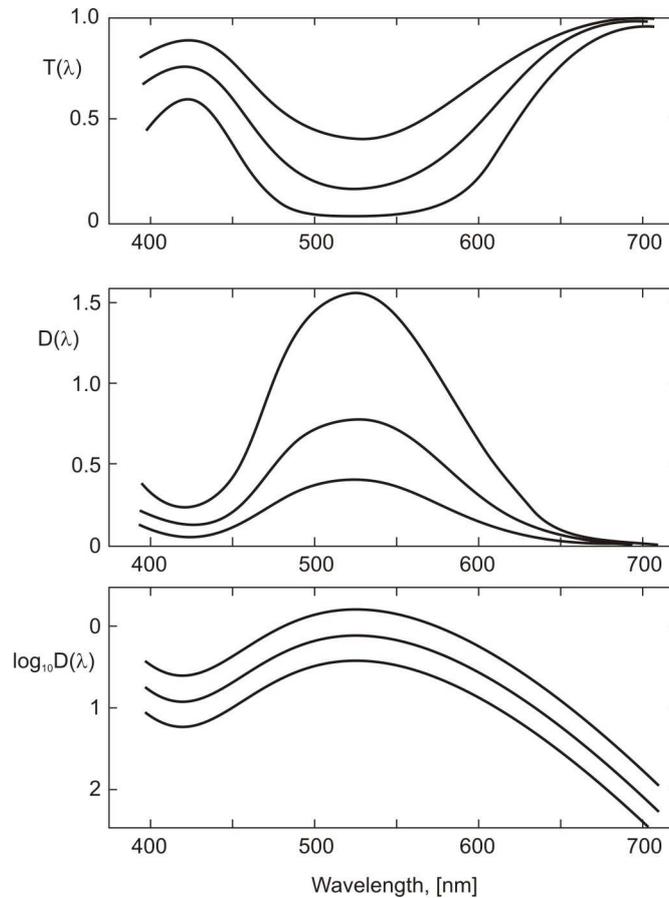

Figure 6: Spectral properties of non-diffusing magenta dye at three concentration - ratios 1 to 2 to 4 times [8]

For mixing of non-diffusing colorant in single transmitting layer the addition of optical density can be applied. The total transmission density of layer with mixture of three different colorants can be calculated as follows:

$$D(\lambda) = D_1(\lambda) + D_2(\lambda) + D_3(\lambda) + D_0(\lambda) \tag{19}$$

where $D_1(\lambda)$, $D_2(\lambda)$, $D_3(\lambda)$ is spectral transmission density of colorants measured without the looses at air/layer interfaces and $D_0(\lambda)$ denote the spectral transmission density attributable to air/layer interface. Colorimetric characteristics can be then obtained by calculating $T(\lambda)$ from

16

D(λ) and using the appropriate illuminant data and standard observer weighting function (color matching function)[8].

3.3.2. *Non-diffusing colorants in transmitting matter in optical contact with diffusing material*

The resultant reflection density of system consisting of transmitting layer and non-diffusing colorant, air gap and reflecting diffuser is equal to double spectral transmission density of colorant layer plus the spectral reflection density of the reflecting surface. The duplication of colorant layer contribution is performed because the light passing though it twice – once it encounter the layer and second when it is reflected back.

If the colored film is not separated from the diffuser by air interlayer the situation is complicated. When the colorant film refractive index is higher than air, total reflection comes into existence and only light within a limited angle can escape. The light passage through the material can be quite complex. Each time the light strikes the diffusing surface it can emerge the sample or may be reflected back. If the colored layer absorption is high the effect of light multiple passages became less significant, however if the absorption is low the effect of multiple internal is reduced only after many passages. Thus low absorptions are more affected by internal reflection than high, which results into widening of absorption bands of colorants.

For a given colorant, thus colored layer that is in contact with difussing reflector will exhibit lower purity and darker appearance than film with the same dye at higher concentration level that gives equal optical density but is not in optical contact. The effect of multiple reflection effect is evident in relationship between reflection and transition density. If reflection density is plotted against transmission density straight line is obtained for colored transmitting layer itself. In case reflecting surface is placed in to contact with the colored layer, the system being more complicated for light passage and thus deflection from linear behaviour at low and also high transmissions densities occur. At low transmission densities the apropriate reflection density is much times higher than the transmission density, then as the multiple internal reflection effect became less important the relationship became linear and at high due to surface reflection instead of reaching the curve only limits the theoretical value of maximum density. The more the surface is glossy the lower maximum value will be reach.

As the effect of multiple internal reflections is depending on absorption level then samples exhibiting spectra with peak(s) of different absorption level will not be affected uniformly and thus hue shift will perceived at higher pigment concentration. With increasing degree of concentration the absorption band will be more broaden at higher absorption level than at

lower. Cyan colorants perform shift towards blue hues with growing concentration because their absorption in greens are more affected.

Colorimetric evaluation of transmitting layers colored by non-diffusing colorants that are in optical contact with diffusing material include calculation of $R(\lambda)$ from calibration dependence of reflectance as a function of transmission and incorporating use of appropriate illuminant and standard observer weighting functions [8].

3.3.3. Layer with light diffusing and absorbing colorants

When pigments are used as colorants or dyes applied on fibres as in textiles, some of the light in addition to being absorbed, is scattered. The dependency of colorant amount and colorimetry became more complex.

Let us analyze the light flux within selected horizontal layer of plan parallel colorant film that is irradiated by diffuse light (see figure 7). Only light channels travelling up and down are considered because the light that travel parallel to the layer boundaries is negligible as for every amount of light passing in one direction, equal amount going in opposite direction exist. Further, any light flux could be divided into horizontal and vertical components and ignoring horizontal only vertical will be studied.
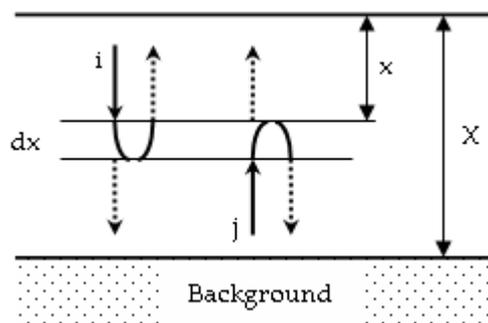

Figure 7: Two-fluxes Kubelka-Munk model

The entire thickness of ink film is denoted by X, and the vanishingly thin layer which is situated in distance x from the surface has thickness dx. The light flux travelling downwards will be symbolized i, the amount going upwards j. At distance x from the surface these two channels will have intensity i_x and j_x. The light passing through the element is decreased by absorption Kdx and scattering backwards Sdx. (K denotes absorption and S scattering coefficients). The light absorbed is lost. The light from channel i is scattered backward into direction j and thus lost of flux i due to scattering is added to flux j. The same is true for photons coming from the bottom of dx. Quantifying the changes in each flux gives the following:

$$di_x = -Ki_x dx - Si_x dx + Sj_x dx \tag{20}$$

$$-dj_x = -Kj_x dx - Sj_x dx + Si_x dx \tag{21}$$

The negative signs in the j_x is due to j flux goes in channel opposite to x. Dividing the expression by dx results in:

$$di_x / dx = -(K + S)i_x + Sj_x \tag{22}$$

$$dj_x / dx = -Si_x + (K + S)j_x \tag{23}$$

Let us define reflectance radio r_x which is proportion of upwards and downwards fluxes:

$$r_x = j_x / i_x \tag{24}$$

The changes of r_x with position in the layer is found by differentiating its formula with respect to x:

$$\frac{dr_x}{dx} = \frac{i_x \dfrac{dj_x}{dx} - j_x \dfrac{di_x}{dx}}{i_x^2} \tag{25}$$

By establishing the equation 22 and 23 and editing we obtain:

$$\frac{dr_x}{dx} = -Sr_x^2 + 2(K + S)r_x - S \tag{26}$$

Then the integral

$$-S \int dx = \int \frac{dr}{r_x^2 - 2\dfrac{K + S}{S} r_x + 1} \tag{27}$$

can be solved by setting boundary condition:

$$x = X, \, r_x = R \quad \text{and} \tag{28}$$

$$x = 0, \, r_x = R_g \tag{29}$$

to give general expression:

$$\ln \frac{(R - a - \sqrt{a^2 - 1})(R_g - a + \sqrt{a^2 - 1})}{(R_g - a - \sqrt{a^2 - 1})(R - a + \sqrt{a^2 - 1})} = 2SX\sqrt{a^2 - 1} \tag{30}$$

where $a = 1 + (K/S)$, R is reflectance of the film of thickness X and R_g is reflectance of substrate on which the layer lies.

This description is known two constant Kubelka-Munk (KM2) because of the coefficient S and K being determined separately.

If we consider the layer to be so thick that further increases of X will not have significant effect on its reflectance, then the reflectance ratio r_x will not be function of x. The reflectance R_∞ can be found by setting X in formula (30) to be equal ∞, then the equation (30) become:

$$R_\infty = 1 + \frac{R}{S} - \sqrt{\frac{R^2}{S^2} + 2\frac{R}{S}} \qquad (31)$$

Or the more familiar inverse expression referred as single constant Kubelka-Munk theory:

$$\frac{K}{S} = \frac{(1-R_\infty)^2}{2R_\infty} \qquad (32)$$

All these expression needs to be tread for each wavelength separately.

For colorant mixture, the absorption and scattering coefficients were tested to be additive [27, 28]:

$$\frac{K}{S} = \frac{c_1 K_1 + c_2 K_2 + \cdots + K_g}{c_1 S_1 + c_2 S_2 + \cdots + S_g} \qquad (33)$$

Where c is colorant concentration, K_q, S_q are absorption and scattering coefficient of component q and substrate g respectively.

Kubelka-Munk formula relates the resulting reflectance of system comprising of colorant mixture with properties of each layer. The determination of K, S konstant can be in some situation quite complex, however, as shown above in limit cases simplification can be achieved. There are three possible ways of application Kubelka-Munk theory in reflectance prediction: single constant, relative two constant and absolute two constant methods [2, 4, 8, 9, 29, 30].

Single constant theory (KM1)

In a single constant approach, reflectance is solely function of K/S rather than absolute numerical values K and S. The KM1 variation can be advantageously used in prediction of dye and textile or opaque pigmented layers containing colorant with scattering coefficient in combination to materials with such as white base paint. The absorption of mixture grows proportionally with increasing level of CB. But as the K of CB is much higher than the S the characteristics of the resulting material will not be altered. The K/S fraction is directly proportional to the amount of CB added.

The nonlinear dependency in equation (31) explains the fact that pure white pants is very sensible to color impurities. The slope of dependency between K/S and R plotted in logarithmic scale, that is this measure of physical sensation, is close to ideal white ($R = 1$) considerably steeper than in area of technical white ($R = 0.8 – 0.5$).

Other situation where single constant approach can be used include transparent lacquers, varnishes, plastics films… Printing inks cannot be treat altogether as their compositions varies according to the printing technique which they are designated for. For most single constant is adequate when absorption coefficients are determined for set of concentration. The light scattering in printed samples is assumed to originate from paper as mentioned in capture 2. 4. and/or white pigment if presented in ink formulation [2].

Single constant approach (KM1) for reflectance prediction of transparent ink film

In 1940s Duncan has showed that K/S function is additive. For printing ink color work the scattering is considered to come from substrate and white ink. If no white or other highly scattering the equation 33 can be write as follows:

$$K/S = c_1 K_1/S_{sub} + c_2 K_2/S_{sub} + \ldots + (K/S)_{sub} \tag{34}$$

in which c_1 is concentration of appropriate ink in mixture and subscript symbolize the substrate. For opaque film the concentration is related to the total pigment volume:

$$c_1 + c_2 + \ldots = 1 \tag{35}$$

For non-opaque layers also the amount of vehicle c_v has to be considered:

$$c_1 + c_2 + \ldots + c_v = 1 \tag{36}$$

Application of equation (34) for prediction reflectance of resulting mixture

1. Determination of $(K/S)_{sub}$ from paper reflectance spectra according eq. 32

2. Similarly K/S of films containing only one transparent pigment is established according eq. 32. Then according eq. 34 the K_i/S_{sub} for each colorant can be calculated as follows:

    $$K_i/S_{sub} = (K/S - (K/S)_{sub})/c_i \tag{37}$$

3. The K_i/S_{sub} are then employed in equation 34 to gain K/S of the mixture and with application of formula 32 reflectance prediction of mixture can be made.

Single constant approach (KM1) for reflectance prediction of opaque ink film

If white or other highly scattering pigment is incorporated in ink formulation the calculation are more complex as the scattering properties of white ink must be taken unto account together with the substrate. The equation 33 is modified:

$$K/S = (c_1 K_1 + c_2 K_2 + \ldots)/ (c_w K_w) + (K/S)_w \tag{38}$$

Where K_w and S_w are the absorption and scattering coefficient of standard white pigment, c_w is its concentration. Analogous to transparent film $c_1 + c_2 + \ldots + c_w = 1$.

Prediction of opaque-ink-film reflectance according equation no. 38:

1. From reflectance of layer containing only white pigment the $(K/S)_w$ is calculated with use of expression 32

2. Similarly *K/S* value of film consisting of white plus tinting pigment is determined based on reflectance measurement and formula 32

3. The resulting K/S coefficinent is used to calculate K_i/S_w value according:

$$K_i / S_w = [K / S - (K / S)_w]/[c_i / (1 - c_i)] \qquad (39)$$

In which $c_i + c_w = 1$.

K_i/S_w is then used in equation (38) to determine the *K/S* of resulting mixture and with use of eq. 32 prediction of reflectance can be made.

The theory (eq. 30) when the two constant are determined separately is usually called two–constant Kubelka-Munk equation. Further, there are two approaches to use the theory to prediction the reflectance: relative and absolute. In the relative two constant model optical properties of each colorant are specified in relation to standard white base and apply to opaque layer such as paint, plastics.

In case of absolute two constant method the colorants are characterized by absolute absorption and scattering constants. It can be used in assessment of both the opaque and the transparent and translucent layers on substrate [29, 30].

Kubelka-Munk coefficients K and S

The Kubelka-Munk coefficients are defined in terms of reflectance and transmittance of thin layer. To link *K* and *S* to optical properties of material separate model is needed. The absorption coefficient can be obtain as follows:

$$K = 2\varepsilon \qquad (40)$$

However, characterization of *S* is more complex. The simplest Kubelka's approach is based on assumption that the radiation is isotropically scattered by each particle and only half of total light will be scattered into upper hemisphere and thus will affect the layer reflectance. Thus:

$$S = \sigma \qquad (41)$$

In which ε is absorption and σ is scattering coefficient per unit path length of material.

Accuracy of Kubelka-Munk theory

Kubelka-Munk is two-fluxes simplification of multi-flux radiation transfer process. Verification of KM prediction is quite tricky due to experimental setup that will match all the restrictions applied during theory derivation. It was found that the predicted value R_∞ are correct only when $R_\infty = 0$ or $R_\infty = 1$ in other cases deviation up to 8 % occurs.

The disagreements in reflectance were investigated by several authors. Mudgett and Richards in their study of the relationship between K, S, ε, σ suggested that the differences can arise from assumption that coefficients K and S are same for the downward (i) and upward (j) flux. Based on multi-flux analyse they pointed out this assumptions to be of limited accuracy. Even under diffuse illumination and isotropic scattering the two upwards and downwards flux will vary. Then eqs. 22 and 23 become:

$$di_x / dx = -(K_i + S_i)i_x + S_j j_x \tag{42}$$

$$dj_x / dx = -S_i i_x + (K_j + S_j)j_x \tag{43}$$

Further, they showed that the two scattering coefficient can be replaced by single one S. The re-established two constant theory corrects the previously adopted simplification that forward and reverse flux have the same angular distribution, but it is still assumed that the respective angular distribution is consistent through the sample. The issue of non-uniformity distribution of diffuse flux within the layer is most pronounced in assessment translucent media [1].

Kubelka [31] further developed the question of optics of non-homogenous layers whose scattering and absorption coefficient vary vertically within the media. He found that the original equations still apply, however the K and S constant is now function of vertical position in the layer. In his paper he concluded that reflectance and absorption of non-homogenous specimen depends on direction of illumination, whereas transmission does not.

In the Kubelka-Munk theory reflectance and transmittance of material is considered without looses at the boundaries. Colored layers made bellow CPVC form a planparaler thin slice where the pigments lie beneath the surface of vehicle. Due to the discontinuity in refractive index at the boundary a portion of the incident light will be reflected. The amount reflected depends on refractive index, light polarization and angle of incidence and the reflected ray follows the Fresnell's equations. Calculations have been published by number of authors, the most know is Saunderson correction [32]:

$$R' = \frac{(1 - k_e)(1 - k_i)R_s}{(1 - k_i R_s)} + k_e k$$

where R' is measured reflectance, R_s is corrected reflectance used in Kubelka-Munk theory, $k_e = (n - 1)^2/(n + 1)^2$ and denote top surface reflection, $k_i = 0.68–0.56$ is internal reflectance at top surface, n is refractive index of the medium and k is proportion of external reflection registered by instrument (if specular component is included $k = 1$, if excluded k is zero) [29].

4.   Application of PA to colored material evaluation

4.1.   Theory of photoacoustic effect in condensed media

First theories were proposed in 19th century by Bell who supposed air expulsion from pores to take place during heating. Rayleigh suggested that the signal arises primary from the thermally induced mechanical vibration of solid. Finally, Mercadier and Preece came with the concept of PA signal arising from the periodic heating at solid-gas boundary that is closed to modern conception of photoacoustic signal generation. However, Rayleigh and Bell mechanisms also contribute.

Parker [33] performed first theoretical evaluation of photoacoustic effect in the twentieth century. He observed measurable PA signal arising from cell window while carry out experiments with gases. His findings applied for polished surfaces of transparent glass.

Theory, that is more general has been derived by Rosencwaig and Gersho who studied condensed media that is in contact of backing material placed in cylindrical cell (see figure 8). The cell has diameter D and length l that is in comparison with generated acoustic wave small. Registration microphone placed in the wall of the cell detects the average acoustics signal that arises from the gas disturbance in the cell. The sample having circle profile and thickness l is mounted on not light absorbing and poorly thermally conducting material with thickness l''. The gas is also supposed to be non-absorbing of light.
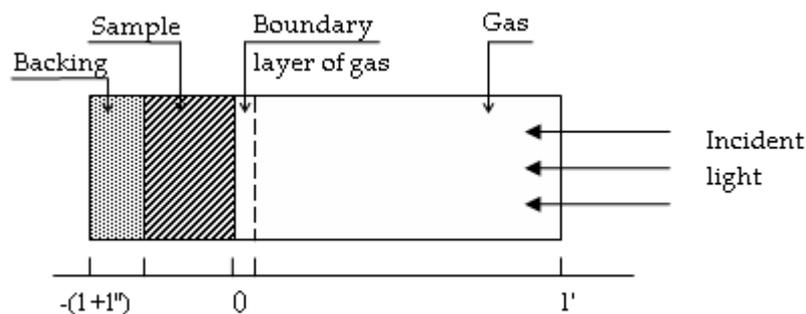

Figure 8: Schema of considered photoacoustic cell [33]

They suppose the PA signal depends both on its generation at sample-gas interface which is given by periodic temperature changes at boundary and the disturbance transfer through the gas towards the microphone. Following parameters will be used to characterize the PA phenomena:

Table 1: Parameters used in description of photoacoustic response

Denotation	Dimension	Term
I_0	W/m²	Incident monochromatic light flux
ω	rad/s	Chopping frequency
ρ	kg/m³	The density
β	m⁻¹	Optical absorption coefficient
μ_β	m	Optical absorption length
α	m²/s	Thermal diffusivity
a	m⁻¹	Thermal diffusion coefficient
μs	m	Thermal diffusion length
C	Cal/g-°C	Specific heat
κ	W/mkg	Thermal diffusivity

Let us consider a sinusoidally modulated monochromatic light with angular frequency $\omega = 2\pi f$ impinging on the sample with intensity *I*:

$$I = \frac{1}{2} I_0 \left(1 + \cos \omega t\right) \tag{45}$$

Thermal diffusion in the solid $(-l \leq x \leq 0)$ is characterized by

$$\frac{\partial^2 \theta}{\partial x^2} = \frac{1}{\alpha} \frac{\partial \theta}{\partial t} - A e^{\beta x} (1 + e^{i\omega t}) \tag{46}$$

with

$$A = \frac{\beta I_0 \eta}{2\kappa} \tag{47}$$

Where θ denote the temperature and η is the efficiency of non-radiative de-excitation by heat. At room temperature η is assumed to be unit for luminescently and photochemically inactive solid.

In solving equation (46), boundary condition are obtained from requirement of temperature and heat flux continuity at boundaries. Further, the temperature at cell walls is assumed to be equal to ambient and dimension of cell being small so that the connective heat flow at gas will be negligible. The complex amplitude of periodic temperature changes at solid-gas interface related to thermal, geometric and optical parameters of the system is given by:

$$\theta_0 = \frac{\beta I_0}{2\kappa(\beta^2 - \sigma^2)}\left[\frac{(r-1)(b+1)e^{\sigma l} - (r+1)}{}\right] \tag{48}$$

In which

$$b = \frac{\kappa'' a''}{\kappa a} \tag{49}$$

$$g = \frac{\kappa' a'}{\kappa a} \tag{50}$$

$$r = (i-1)\frac{\beta}{2a} \tag{51}$$

$$\sigma = (1+i)a \tag{52}$$

The temperature changes in the gas that are thought to be primary source of PA signal are given by the sinusoidal component (a. c.) of the general solution of thermal diffusion equations and can be express as following:

$$\theta_{a.c}(x,t) = \theta_0 e^{-\sigma' x} e^{i\omega t} \tag{53}$$

The equation (53) shows that the time dependent temperature changes in the gas diminish with increasing distance from the sample surface and at length of $2\pi\mu_g$ limits zero. The periodic temperature variation in the sample thus evokes temperature changes only in the boundary layer which expands and contracts cyclically and squeeze on the rest of gas column in the cell as an acoustic piston. Supposing adiabatic gas ($PV^\gamma = constant$) the pressure in the cell due to displacement of gas piston can be gain by:

$$\delta P(t) = Q e^{i(\omega t - \pi/4)} \tag{54}$$

Where $Q = \frac{\gamma P_0 Q_0}{\sqrt{2} l' a' T_0}$ denotes the complex envelope of the sinusoidal pressure variation. The actual physical pressure variation reaching the registration microphone are given by real part:

$$\Delta p(t) = q\cos\left(\omega t - \psi - \frac{\pi}{4}\right) \tag{55}$$

where

$$Q = Q_1 + iQ_2 = q e^{-i\psi} \tag{56}$$

With regard to 48 we can write:

$$Q = \frac{\beta I_0 \gamma P_0}{2\sqrt{2} T_0 \kappa l' a' (\beta^2 - \sigma^2)} \times \frac{(r-1)(b+1)e^{\sigma l} - (r+1)(b-1)e^{-\sigma l} + 2(b-r)e^{-\chi l}}{(g+1)(b+1)e^{\sigma l} - (g-1)(b-1)e^{-\sigma l}} \tag{57}$$

The complex description of generated PA signal is somewhat difficult to interpret; however, simplification can be obtain in limiting cases. Based on the optical properties, samples are gathered into two groups that differ by the relation of optical absorption length to thickness of solid. According to ratio between thermal diffusion and optical length and sample thickness three cases are distinguished in each category. For evaluation of Q in these six cases (see figure 9) is assumed $g < b$ and $b \sim 1$, i.e. $\kappa'a' < \kappa''a''$ and $\kappa'a' \cong \kappa a$ and $(\gamma P_0 I_0 / 2\sqrt{2} T_0 l')$ is replaced by Y.
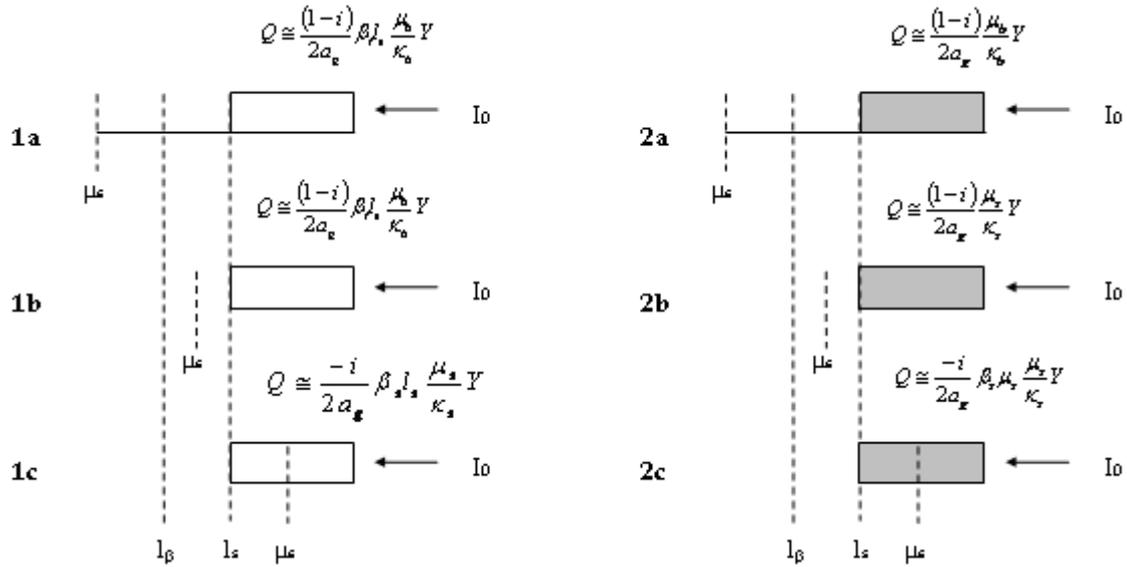

Figure 9 : Six special cases of Rosencwaig and Gersho theory

Optically transparent samples are characterized by absorption through whole sample thickness and some of the light is transmitted through. The acoustics pressure is related to optical absorption coefficient and varies with modulation frequency. Thus changing the chopping frequency enable us to study optical absorption depth profile.

If the sample is thermally thin, Q depends on properties of backing material. When sample is thermally thick, the signal is proportional to β_μ rather than β_l and thus although the light being absorbed in the whole solid, only that absorbed in the first thermal diffusion length contributes to the signal.

The optical opaqueness of solid implies the light being absorbed within very small volume of the sample and none transmitting through.

For situations where $\mu \gg l_\beta$ and $\mu > l_\beta$ (cases 2a and 2b) the response is independent of β. This instance is so-called photoacoustic opaqueness and the resulting PA signal match the spectral characteristics of light source. This case apply for very absorbing samples such as CB. Measurement at these conditions is utilized for normalization of PA response. The expression for Q in these two situations differs only by the thermal parameters – in case 2a that of

backing is employed, whereas in 2b those of solid instead. For thermally thick and optically opaque sample 2c the PA signal again depends on β and thus photoacoustics spectroscopy is unique utility for spectral characterization of highly optically opaque solids [33].

The theory has been tested experimentally verified and showed to be sufficient for many application, however, modification for light scattering is required [6].

4.2. Effect of Particle size on Photoacoustic response

Davidson and King [6] carry experiments with potassium ferricyanide and potassium chromate. They observed gain in PA amplitude with particle size reduction. Reflectance measurement showed that for both samples increase in particle size led to light absorption enhancement.

The observed decrease in absorption with decrease of particle size corresponds with fact that these two compounds act as weak absorbers which are characterized by visual decrease in the color as particle size fall down. In contrast both potassium compounds exhibit gain in PA amplitude with particle size decrement, which indicate light scattering not, being the dominating factor.

Obviously Kubelka-Munk approach is applicable for reflectance measurement potassium ferricyanide and potassium chromate and also to PA measurement of strong absorbers. But is not sufficient to explain PA response of presented weak absorbers. Variation in particle size has a little effect on light absorption but will affect the heat transfer from the sample to surrounding gas which determine the photoacoustic signal since the smaller the particle the greater the surface area [6].

The energy transfer issue was more developed by Belton and Wilson [35]. In Rosencwiag and Gersho theory the generation of acoustic signal is given by the process in which the incident light is absorbed and subsequent de-excitation mechanism in which the energy is converted to heat. In homogenous materials the light absorption can be characterised by Lambert-Beer law and energy transfer is by thermal conduction to the gas in the cell. In powders light scattering comes into existence and Lambert Beer law is no longer valid, also the energy transfer is more complex. The Rosencwaig-Gersho theory suppose the period expansion and contraction of the boundary layer to be primary source of photoacoustic pressure. Helander [34] described that increase in photon density near surface which is caused by light scattering effect can increase the thermal term in the energy transfer process. Explanation of this phenomena provide analyse of heat flow through the composite body – when most of the light energy is concentrated near sample surface there is shorter path length for energy transfer and hence the transfer process is more efficient. As smaller particles generally exhibit greater scattering, PA response enhancement can be

expected on the Helander assumptions of photon cumulation near sample surface. Yang and Fateley reported: the smaller the particle size the higher particle surface to volume ratio and better contact between gas and sample, thus efficient energy transmission to microphone. Reduction in particle size also results in porosity growth, which leads to enhancement of the photoacoustic signal.

Further important aspect is the ratio of particle radius and thermal diffusion length. When the proportion is equal or smaller than unite then the whole particle lying within the thermal diffusion length contribute to PA response. Consequently if the ratio exceeds, only part of the particle that falls into thermal diffusion length of the surface will have the effect on signal generation.

Yang and Fateley [35] claim that ratio of particle diameter to thermal diffusions length is more correct. In their concept when the thermal diffusion length is shorter than particle diameter, they assumed the light entering only from one direction and heating travelling to the unilluminated surface. However, this is of limited accuracy as light scattering comes into play which causes that particle will be illuminated from all directions and thus consideration of radius rather than diameter is more suitable.

Belton et al. [35] performed experiments with CB, sucrose and mixture consisting sucrose and potassium bromide. The signal intensity decreased with growing particle size and exhibit exponential dependency for all studied samples. The general trend observed was similar to that reported by Yang and Fateley. Results, especially on CB where all the light is absorbed in short distance in compare with thermal diffusion length, clearly indicate that the connection between PA response and particle size is general and independent of ratio of particle radius to thermal diffusion length.

Evaluation of correlation between signal intensity and sample porosity exhibit linear relationship, thus implying the energy transfer efficiency gains with higher porosity [35].

4.3. Effect of light scattering on photoacoustic response

In photoacoustic spectroscopy two sort of light scattering effect is distinguished. First in which the light scattered strike the cell wall where is absorbed. Second which deals with internal scattering in the sample. This phenomenon re-distributes the photon density and thus affects the thermal diffusion and PA signal.

The effect of internal scattering on PA response has been mathematically treated by Helander et. al. [5] who studied water solution of dye with addition of latex spheres as scattering elements. He found his derivation on characterization of photon density. As light scattering comes into play the photon distribution is shifted towards the surface of sample causing the

energy transfer from the light absorption to heat be more efficient at the sample surface than deeper in the sample. To evaluate the photon density we introduce a distribution function $f(r,p,t)$ such as that $f(r,p,t)drdp$ is number of particles in volume $drdp$ at point r, p at time t. Photon distribution function in light scattering medium following Morse and Feshbach is given by:

$$\frac{\delta f}{\delta t}(z,\theta,t) = -c\cos\frac{df}{dz}(z,\theta,t) - \beta_t c f(z,\theta,t) + \frac{\beta_s c}{2}\int_{\theta=0}^{\pi} f(z,\theta',t)\sin\theta'd\theta' \tag{58}$$

Where the appropriate form of $f(\bar{r},\bar{p},t)$ is $f(z,\theta,t)$. β_s is scattering coefficient, θ characterise the angle at which the photon is travelling and the $\rho(z,t) = \int_{\theta=0}^{\pi} f(z,\theta',t)\sin\theta'd\theta'$ denotes the photon density in the ordinary space. The equation (58) has been solved with many presumptions in each step including sample being semi-infinite and covering the region $z > 0$, photon net flow being in z direction owing to the homogenous illumination of the plane $z = 0$ and neglecting some insignificant contributions. Further in estimating diffuse photons due to incident light beam assumption that all photons scattered at least one time belong to diffuse photon density. This is not completely true because some direction are more likely and thus multiple scattering is required for the photon direction to be independent of that original. However, there is no net flow due to incomplete scattering.

Integration constants for the diffuse part of photon density are determined by the boundary conditions: at $z = 0$ the only flux in the positive z direction is due to the incident beam and light reflected internally at the water/air interface due to difference in refractive index. And no diffuse disturbance from region $z < 0$ exist. However, to calculate r the part of light reflected at the boundary that is part of the integration constant. And even if the value of r is known the integration constant will be only approximation since neglecting of come contribution were performed during derivation.

Adding the part due to incident bean not yet absorbed or scattered $I_0 = e^{-\beta_t z}/ch\nu$ to diffuse part of photon density gives us total photon density:

$$\rho_t(z) = \frac{I_0 e^{-\beta_t z}}{ch\nu} + \frac{3I_0}{ch\nu(1 - 3\beta_a/\beta_s)}\times\left\{\frac{1+\Delta}{1+\Delta(3\beta_a/\beta_s)^{0.5}}\exp\left[-\left(\frac{3\beta_a}{\beta_s}\right)^{0.5}\beta_t z\right] - \exp(-\beta_t z)\right\} \tag{59}$$

Where β_a is absorption coefficient, h denotes Planck constant, ν is photon frequency, I characterize the incident light and $\Delta = \frac{2}{3}(1+2r)$ in which r are photons reflected at the boundary.

If we calculate the total number of photons per unit in sample by integrating the eq. (59) over z and compare with value for non scattering sample it can be seen that light scattering lower the number of photons in sample. However, PA signal is also affected by their distribution.

To calculate the effect of light scattering on amplitude of PA signal the heat conduction equation for the sample with the power production $P(z)$ corresponding to $\rho_t(z)$ in equation (59) according to

$$P(z) = h\nu\beta_a c\rho_t(z) \tag{60}$$

has to be solved.

Again, presumptions as before including semi-infinite sample, no heat loose to air is consider taking place in calculation of the surface temperature. The heat conduction is given by:

$$T(z) = Ce^{-az} + a_1 \exp\left[-\left(\frac{3\beta_a}{\beta_s}\right)^{0.5}\beta_t z\right] + a_2 \exp(-\beta_t z) \tag{61}$$

where

$$a_1 = \frac{\dfrac{\beta_a A_0}{\kappa}}{\dfrac{\beta_t^2 3\beta_a}{\beta_s} - a^2} \tag{62}$$

$$a_2 = \frac{\dfrac{\beta_a B_0}{\kappa}}{\beta_t^2 - a^2} \tag{63}$$

$$A_0 = \frac{3I_0}{1 - 3\beta_a/\beta_s}\frac{1+\Delta}{1+\Delta\sqrt{3\beta_a/\beta_s}} \tag{64}$$

$$B_0 = I_0\left(1 - \frac{3}{1 - 3\beta_a/\beta_s}\right) \tag{65}$$

and T denote the change of in temperature in the sample due to light absorption. By applying boundary conditions, the surface temperature can be described by:

$$T(0) = \frac{I_0\beta_a}{\kappa a} \times \left\{\frac{3(1+\Delta)}{(1-3\beta_a/\beta_s)\left[1+\Delta\sqrt{3\beta_a/\beta_s}\right]\left[\beta_t\sqrt{3\beta_a/\beta_s}1+a\right]} + \frac{1}{\beta_t+a}\left(1 - \frac{3}{1-3\beta_a/\beta_s}\right)\right\} \tag{66}$$

With absence of light scattering, the temperature can expressed:

$$T(0) = \frac{I_0\beta_a}{\kappa a(\beta_a + a)} \tag{67}$$

As the sample surface temperature directly affect the generated signal ratio R that express photoacoustics signal with and without light scattering can be calculated as following:

$$R = \left(\beta_a + a\right) \times \left\{ \frac{3\left(1+\Delta\right)\beta_s^2}{\left(\beta_s - 3\beta_a\right)\left[\sqrt{\beta_s} + \Delta\sqrt{3\beta_a}\right]\left[\beta_t\sqrt{3\beta_a} + a\sqrt{\beta_s}\right]} + \frac{1}{\beta_t + a}\left(1 - \frac{3\beta_s}{\beta_s - 3\beta_a}\right)\right\} \quad (68)$$

where

$$a = \sqrt{\frac{j\pi f\omega\gamma}{\kappa}} \quad (69)$$

The theory has been experimentally tested by authors and they conclude that simple photon diffusion theory with proper boundary conditions at the sample surface explains the effect of light scattering [5].

5. Conclusions

In a daily life materials that absorb or scatter or transmit light are found. To predict color of object from amount and type of components, theory that will link optical properties with fundamental properties of elements is required. Kubelka-Munk approach is widely used in color-using industry. However, Kubelka Munk method is two-fluxes approximation of the multi flux radiative transfer calculation, thus more exact theories and correction of original Kubelka equation that take into account boundary reflection have been reviewed by many authors.

Photoacoustics and photoacustic spectroscopy are non-destructive methods for study optical and thermal properties of sample in different depths beneath the sample surface. It enables to obtain absorption spectra of powders, suspensions, emulsions and other light scattering materials where conventional measurements fail. The theory of photoacoustics effect was derived by Rosensweig and Gersho. The effect of internal light scattering within the sample and its effect on photoacoustics response was treated by Helander at al. Their explanation of growth of PA signal has been made by calculation of photon density in the sample.

References

[1]   Nobbs J.: *Rev. Prog. Coloration* **15**, 66 (1985).

[2]   Kubelka P., Munk F.: *Z. tech. Phys*. **12**, 593 (1931).

[3]   Mudget P. S., Richards L. W.**:** *Appl. Optics* **10**(7), 1485 (1971).

[4]   Kang H. R.: *IS&T/SID Color Imaging Conference*: Scottsdale, Arizona, 1993, p. 78.

[5]   Helander P., Lundström I., McQueen D.: *J. Appl. Phys*.: **51**(7), 3841 (1980).

[6]   Davidson R.S., King D.: *Anal. Chem.*: **56**(8), 1409 (1984).

[7]   Tilley R. J. D.: *Colour and Optical Properties of Materials*, John Wiley & Sons, 1999.

[8]   Hunt R. W. G.: *Measuring Colour*, Fountain Pr Ltd, 2001.

[9]   G. Sharma: *Digital color Imaging*, CRC, 2002.

[10]   Green P., MacDonald L.: *Colour Engineering: Achieving Device Independent Colour*
        John Wiley & Sons, 2002.

[11]   Otahalova L., Green P. J., Johnson A. J.: Sample backing in graphic arts colour
        measurements, unpublished paper.

[12]   Callahan F. P Jr.: *J. Opt. Soc. Am.* **42**, p. 104 (1952).

[13]   Judd D. B.: *J. Research Natl. Bur. Standards* **29**, p. 329 (1942).

[14]   Clapper F. R. Yule J. A. C., *J. Opt. Soc. Am.* **43**, p. 600 (1953).

[15]   Keen B. A., Porter A. W.: *Roy. Soc. Proc A* **89** (612), 370 (1914).

[16]   Rayleigh J. W.: *Proc. Roy. Soc. Ser. A* **90** (617), 219 (1914).

[17]   Green P.: *Understanding Digital Color*, Graphic Arts Technical Fndtn, 1999.

[18]   Jayasuria S., Moore C., Ruehle T.: *Ink world*, **12**(2), p. 28 (2006).

[19]   Lee H.-K., Joyce M.K., Fleming P.D.: *J. Imaging Sci. Technol*. **49**(1), 54 (2005).

[20]   TAPPI standard, T480 m51.

[21]   Lee H.-K., Joyce M.K., Fleming P.D.: *NIP19: International Conference on Digital Printing
        Technologies*, New Orleans, LA, 2003, vol. 19, p. 613.

[22]   Lee H.-K., Joyce M.K., Fleming P.D., Cameron J.: *Proc. TAPPI Coating Conference*,
        Atlanta, GA, 2002 (electronic distribution).

[24]   Brown T. J.: *Ink maker* **82**(3), 23 (2004).

[23]   Preston J. S., Parsons D. J., Gate L. F., Husband J. C., Legrix A., Jones M.: *Journal of
        Graphic Technology* 1(2), 29 (2003).

[25]   http://www.specialchem4coatings.com/tc/color/index.aspx?id=opacity.

[26] http://www.millenniumchem.com.

[27] Ducan D. R.: *Proc. Roy. Soc. London* **52**, p. 380 (1940).

[28] Persoz B.: Peintures, pigments, vernis, **21**, p. 329, (1945).

[29] Johnoson T. : Non-process ink recipe formulation, company research.

[30] H. R. Kang: *Color Technology for Electronic Imaging Devices*, SPIE, 1997

[31] Kubelka P.: *J. Opt. Soc. Am.* 44(4), 330 (1954)

[32] Saunderson J. L.: *J. Opt. Soc. Amer.* **32**, 727 (1942)

[33] A. Rosencweig: *Photoacoustics and Photoacoustic Spectroscopy*, John Wiley & Sons, 1980, Chem. Analysis, vol. 57.

[34] Helander P.: *J. Appl. Phys* **54** (6), 3410 (1983)

[35] Belton P.S., Wilson R.H., Saffa A.M.: *Anal. Chem.:* **59**(19), 2378 (1987)

List of abreviation

HSP   hollow sphere pigments

CPVC   critical pigment volume concentration

KM   Kubelka-Munk

KM 2   Kubelka-Munk two-constant equation

KM 1   Kubelka-Munk single-constant equation

CB   Carbon Black